EXPERIMENTAL EVIDENCES UNEQUIVOCALLY PROVE THE ROLE OF STEREOELECTRONICS AS ONE OF THE MAJOR FORCES RESPONSIBLE FOR THE SELF-ASSEMBLY OF DNA AND RNA

Parag ACHARYA, Johan ISSAKSON, P. I. PRADEEPKUMAR and
Jyoti CHATTOPADHYAYA*

*Department of Bioorganic Chemistry, Box 581, Biomedical Centre, University of Uppsala,
S-751 23 Uppsala, Sweden; e-mail: jyoti@boc.uu.se*

Three independent sets of experimental evidences are presented here that unequivocally prove the importance of stereoelectronics as one of the major forces, along with stacking, hydrogen-bonding and hydration, in dictating the self-assembly of nucleic acids: (*1*) experimentally obtained thermodynamics of conformational transmission in nucleosides and mononucleotides clearly show the conformational transmission across the nucleotidyl wire (*i.e.* from aglycone to sugar to phosphate) is responsible for modulation of the sugar-phosphate backbone conformation as a result of change of aromatic character of the aglycone in a pH dependent manner, (*2*) single-atom mutation of the endocyclic sugar-oxygen to a methylene group (*i.e.* substitution of 2′-deoxyadenosine moiety to a carbocylic 2′-deoxyaristeromycin in a self-complementary 12-mer DNA) alters the Watson–Crick paired duplex structure to a dynamic equilibrium of Hoogsteen and Watson–Crick paired duplexes in *ca* 1:1 ratio, (*3*) introduction of the North or North-East constrained nucleotides in the antisense strand in the corresponding antisense-RNA hybrid duplex forces a certain stretch of antisense/RNA hybrid duplex to take up a local pseudo RNA/RNA type structure as a result of the conformational transmission from the constrained residue, which is evidenced from the alteration of the RNase H recognition and cleavage properties.

SELF-ASSEMBLY OF DNA AND RNA

The cooperative interplay of pentofuranose, nucleobase and phosphodiester moieties dictates the intrinsic dynamics and architectural flexibility of nucleic acids resulting into its specific function[1]. The stability of the folded structure of nucleic acid leading to its self-assembly and recognition is attributed to the interplay of various forces[1] such as (i) intermolecular hydrogen bonding between complementary nucleobases; (ii) intramolecular base-base stacking interactions; (iii) electrostatic interactions and hydration. However, recent studies[2,3] have unequivocally demonstrated the importance of stereoelectronic forces, besides the above mentioned forces, in the self-organization process of nucleic acids vis-à-vis their biological functions. The physico-chemical roles of the aglycone, sugar and phosphate, depending upon the local microenvironment, dictates the stereoelectronic forces thereby affecting the function as well as the self-assembly of nucleic acid.

We will present here three independent sets of experimental evidences that unequivocally show the importance of stereoelectronics: (*1*) experimental thermodynamics of conformational transmission in nucleosides and mononucleotides[2a–o]; (*2*) single-atom mutation of the endocyclic sugar-oxygen to a methylene group (*i.e.* 2′-deoxyadenosine moiety to a carbocylic 2′-deoxyaristeromycin in a self-complementary 12-mer DNA) alters the DNA polymorphism[11], (*3*) introduction of the N- or N/E-constrained nucleotides in the antisense strand in the corresponding antisense-RNA hybrid duplex alters the RNase H recognition and cleavage properties[20].

1. Experimentally Obtained Thermodynamics of Conformational Transmission in Nucleosides and Mononucleotides

(A) Stereoelectronic Forces – Anomeric and *gauche* Effects

The dynamic interplay of various stereoelectronic *gauche*[2a–e,g,h,n,o,5] and anomeric effects[2g,h,j,l,n,o,3a,4] and associated steric effects energetically drives the two-state pseudorotational equilibrium[2,3,6] between north-type (N, C2′-*exo*-C3′-*endo*) and south-type (S, C2′-*endo*-C3′-*exo*) of the pentofuranose moiety [N ⇌ S, Fig. 1], which in turn is dictated by the electronic nature of the aglycone[2g,n,o,3a] and other substituents on the sugar ring[2a–e,m,3a]. The

North: 3'-*endo*-2'-*exo*
$0° \leq P \leq 36°$
$\Psi_m = 38.6 \pm 3°$

South: 3'-*exo*-2'-*endo*
$144° \leq P \leq 190°$
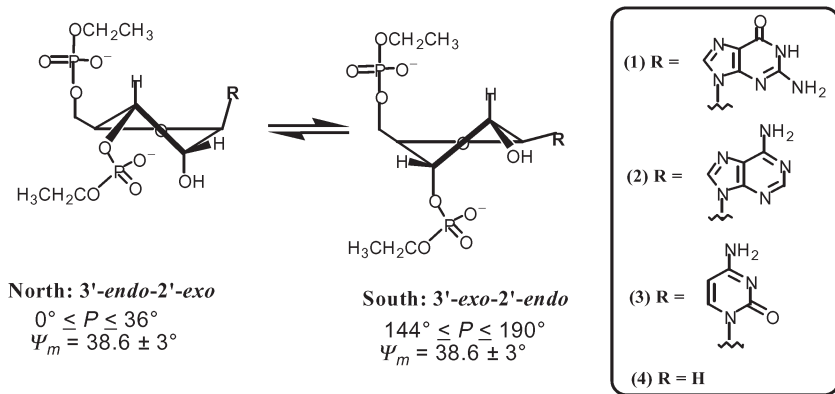$\Psi_m = 38.6 \pm 3°$

(1) R =

(2) R =

(3) R =

(4) R = H

Fɪɢ. 1

Schematic representation of the dynamic two-state North (N) ⇌ South (S) pseudorotational equilibrium[2,3,6] [P = phase angle and Ψ_m = puckering amplitude] of the constituent β-ᴅ-pentofuranose moiety in gaunosine 3′,5′-bisphosphate [EtpGpMe (**1**)], adenosine 3′,5′-bisphosphate [EtpApMe (**2**)] and cytidine 3′,5′-bisphosphate [EtpCpMe (**3**)], as well as their apurinic counterpart [Etp(AP)pMe (**4**)]

aglycone promoted anomeric effect (AE) involving O4′ of the pento-furanose [*i.e.* O4′–C1′–N1/9 atoms, leading to $n_{O4'}$ ($\sigma^*_{C1'-N1/9}$ orbital mixing[2a–e,n,o,3a,4]] drives the sugar conformation towards the N-type pseudo-rotamers. The 3′-substituent X (where X = OH for natural in β-D-nucleotides and X = OPO$_3$H for β-D-nucleotides) promoted *gauche* effect (GE) involving O4′–C4′–C3′–X3′ atoms [leading to $\sigma_{C3'-H3'}$ $\sigma^*_{C4'-O4'}$ orbital mixing[2g,h,n,o,5a]] steers the sugar conformation towards the S-type geometry[2g,h,n–p,3a]. However, 2′-substituent Y (where Y = OH for natural RNA) has GE involving both O4′ of the pentofuranose [*i.e.* O4′–C1′–C2′–Y2′ leading to $\sigma_{C2'-H2'}$ $\sigma^*_{C1'-O4'}$ orbital mixing[2d,g,h,n,o,3a]] and N9/1 of aglycone [*i.e.* N9/1–C1′–C2′–Y2′ leading to $\sigma_{C2'-H2'}$ $\sigma^*_{C1'-N9/1}$ orbital mixing[2d,g,h,n,o,3a]]. It has been found that GE[O4′–C4′–C2′–Y2′] and GE[N9/1–C4′–C2′–Y2′] are counteractive; the former drives the pseudorotational equilibrium of the sugar moiety toward N-type conformation, whereas the later steers it towards S-type conformation. So the preferred sugar vis-à-vis backbone conformation of nucleic acids depends on the culmination of the *mutual interplay* of substituent dependent anomeric and *gauche* effects[2,3]. Figure 2 thus shows the quantitation of *gauche* and anomeric effects in nucleosides, nucleotides and abasic sugars through pairwise comparisons[3] of ΔH^0 of their two-state N $\rightleftarrows$ S pseudorotational equilibria at neutral pH.

(B) Tunable Anomeric Effect

The overall effect of nucleobase is dictated by the steric and stereoelectronic nature of nucleobase[3a] as well as the sugar substitutents[2e,3a]. The pairwise comparison (Fig. 2) in 2′,3′-dideoxynucleosides (β-D-ddN, $\Delta\Delta H_2^0$), 2′-deoxy-nucleosides (β-Δ-dN, $\Delta\Delta H_3^0$) and ribonucleosides (β-D-rN, $\Delta\Delta H_4^0$) shows that pyrimidine aglycone has larger AE at neutral state than purinic counterpart [*i.e.* guanin-9-yl < adenin-9-yl < thymin-1-yl ≈ uracil-1-yl < cytosine-1-yl]. Nucleobase modifications have been used extensively to search for anti-viral and anti-tumor active compounds. The strengthening of AE in 8-aza-3-deazaguanine stabilizes N-type conformation by 3.1 kJ mol^{-1} (at neutral pH) compared to guanine due to the redistribution of electron-density from N9 into the pyridine moiety[8c]. Higher electron-attracting substitution at 7- and 8-position of 7-deaza-2′-deoxynucleosides[8d] steers the sugar conformation more towards N-type pseudorotamers.

Medium-dependent change of electronic character of nucleobase[2g,n,o,3a] such as protonation and/or deprotonation changes the strength of the anomeric effect. Lower electron density at N9/1 of protonated nucleobase enhances $n_{O4'}$ $\sigma^*_{C1'-N1/9}$ orbital interaction, thereby increasing AE, which is manifested with increased preference for the N-type sugar conformation, whereas the reverse is true for deprotonation. Thus the ΔG^0 of N $\rightleftarrows$ S equi-

librium at different pH for nucleoside 3′-ethylphosphates (NpEt)[2r] are as follows: ApEt (–3.2 kJ mol^{-1} at pH 6.6, –1.3 kJ mol^{-1} at pH 1.9, *i.e.* tunability $[\Delta\Delta G^0_{(pH\ 1.9-6.6)}]$ = 1.3 kJ mol^{-1} for N-type conformation), GpEt (–2.6 kJ mol^{-1} at pH 6.6, 0.0 kJ mol^{-1} at pH 1.9, –4.4 KJ mol^{-1} at pH 10.3, *i.e.* tunability $[\Delta\Delta G^0_{(pH\ 1.9-6.6)}]$ = 2.6 kJ mol^{-1} for N-type conformation; tunability $[\Delta\Delta G^0_{(pH\ 10.3-6.6)}]$ = –1.8 kJ mol^{-1} for S-type conformation), UpEt (–0.8 kJ mol^{-1} at pH 6.6, –1.2 kJ mol^{-1} at pH 10.3, *i.e.* tunability $(\Delta\Delta G^0_{(pH\ 10.3-6.6)}$ = –0.4 kJ mol^{-1}
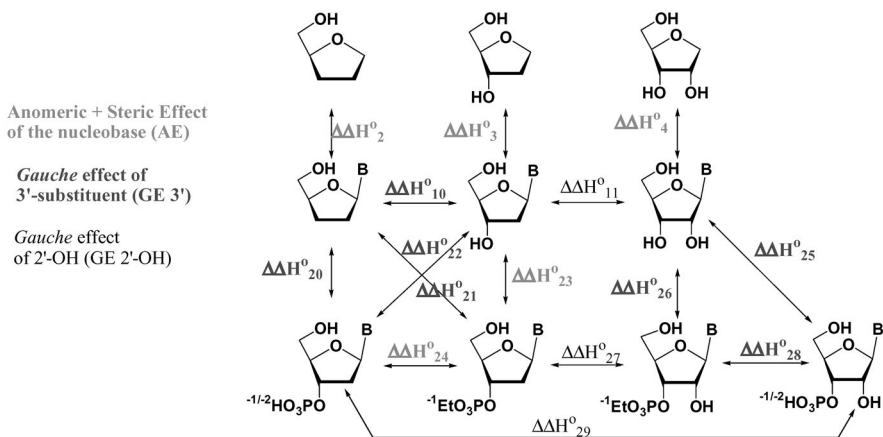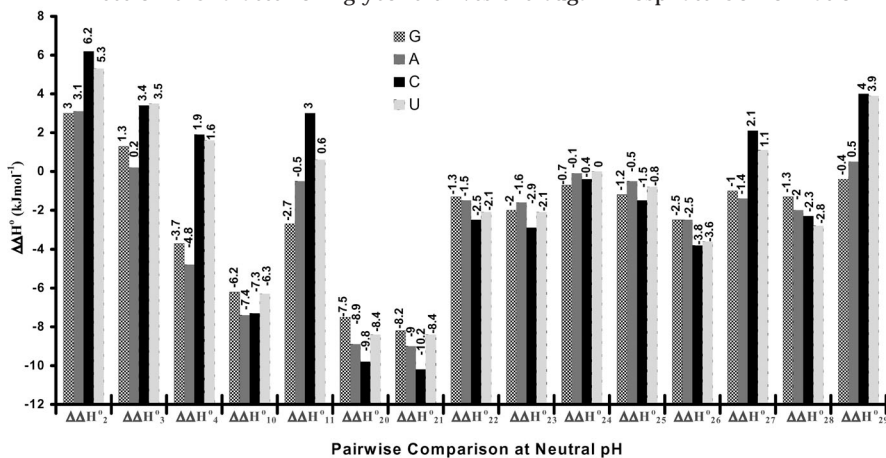

Fig. 2

The quantitation of gauche and anomeric effects in nucleosides and abasic sugars through pairwise comparisons of ΔH^0 of their N $\rightleftarrows$ S pseudorotational equilibria at Neutral pH

for S-type conformation), CpEt (–0.2 kJ mol^{-1} at pH 6.6, 0.6 kJ mol^{-1} at pH 1.9, *i.e.* tunability [$\Delta\Delta G^0_{(pH\ 1.9-6.6)}$] = 0.8 kJ mol^{-1} for N-type conformation). *For comparison, note the tunability* [$\Delta\Delta G^0_{(pH\ 1.9-6.6)}$] *in the corresponding nucleosides (N)*: A (–1.8 kJ mol^{-1} at pH 6.5, –0.5 kJ mol^{-1} at pH 1.2, *i.e.* tunability [$\Delta\Delta G^0_{(pH\ 1.2-6.5)}$] = 1.3 kJ mol^{-1} for N-type conformation), G (–1.5 kJ mol^{-1} at pH 6.4, 1.5 kJ mol^{-1} at pH 0.6, –2.8 kJ mol^{-1} at pH 10.9, *i.e.* tunability [$\Delta\Delta G^0_{(pH\ 0.6-6.4)}$] = 3.0 kJ mol^{-1} for N-type conformation; tunability [$\Delta\Delta G^0_{(pH\ 10.9-6.4)}$] = –1.3 kJ mol^{-1} for S-type conformation), U (–0.3 kJ mol^{-1} at pH 7.3, –0.1 kJ mol^{-1} at pH 11.5, *i.e.* tunability ($\Delta\Delta G^0_{(pH\ 11.5-7.3)}$ = –0.2 kJ mol^{-1} for S-type conformation), CpEt (1.5 kJ mol^{-1} at pH 6.6, 1.9 kJ mol^{-1} at pH 1.2, *i.e.* tunability [$\Delta\Delta G^0_{(pH\ 1.2-6.6)}$] = 0.4 kJ mol^{-1} for N-type conformation). Thus the comparison of $\Delta\Delta G^0$ of NpEt and N clearly shows that the electronegativity of 3′-OH and 3′-phosphate are quite comparable (see below).

pH dependent ^{1}H NMR studies with carbocyclic nucleoside[2m] such as aristeromycin (chemical modification of O4′ with CH$_2$), in comparison with its natural analog, adenosine, showed that electronic nature of aglycone had no effect on the drive of constituent cyclopentane conformation, thereby establishing the role of AE in the drive of the sugar conformation in *N*- and *C*-nucleosides. The S–C–N anomeric effect in 4′-thio-2′-deoxynucleosides[8b] increases in the following order (ΔH^0 in kJ mol^{-1}): thymine (–2.3 at pH 11.9, –2.7 at pH 6.7) < cytosine (–1.6 at pH 2.0, –1.4 at pH 6.5) < guanine (1.1 at pH 0.7, –0.7 at pH 6.7, –0.4 at pH 11.8) < adenine (0.0 at pH 1.8, 0.8 at pH 6.8) [note: this is an opposite order to those of natural nucleosides] and is weaker than the O–C–N anomeric effect[2j] in its natural counterpart (4′-oxonuclosides) at neutral state (ΔH^0 in kJ mol^{-1}): β-D-T (–2.0 at pH 11.2, –1.6 at pH 7.5) ≈ β-D-dC (0.1 at pH 1.3, –0.8 at pH 6.4) > β-D-dG (1.8 at pH 1.0, –2.4 at pH 6.2 and –5.0 at pH 10.9) > β-D-dA (–3.8 at pH 6.1, –1.1 at pH 1.5).

pH-dependent conformational analyses by ^{1}H NMR of *C*-nucleosides[2k,3a] showed the anomeric tunability [in terms of $\Delta\Delta G^0_{P-N}$ and $\Delta\Delta G^0_{D-N}$ (in kJ mol^{-1}), where $\Delta\Delta G^0_{P-N}$ and $\Delta\Delta G^0_{D-N}$ represent the additional stabilization of N-type sugars in the protonated (P) state compared to in the neutral (N) state, and that of S-type sugars in the deprotonated (D) state compared to the N state, respectively] by virtue of the participation of $n_{O4'} \rightarrow \sigma^*_{C1'-C5(sp2)}$ anomeric interactions in *C*-aglycone to drive its N ⇌ S equilibrium. The comparison of this anomeric tunability of *C*-nucleosides with that of *N*-nucleosides show that the anomeric tunability is more pronounced in pyrimidine *C*-nucleosides [Ψ-isocytidine ($\Delta\Delta G^0_{P-N}$: 1.9 kJ mol^{-1} and $\Delta\Delta G^0_{D-N}$: –1.6 kJ mol^{-1}), Ψ-uridine ($\Delta\Delta G^0_{D-N}$: –1.7 kJ mol^{-1}) and 1-Me-Ψ-uridine ($\Delta\Delta G^0_{D-N}$: –0.8 kJ mol^{-1})]

than that of pyrimidine *N*-nucleosides [β-D-C ($\Delta\Delta G_{P-N}^0$: 0.4 kJ mol⁻¹); β-D-U ($\Delta\Delta G_{D-N}^0$: –0.2 kJ mol⁻¹)], whereas there is no significant difference between purine *C*-nucleosides [9-deaza-adenosine ($\Delta\Delta G_{P-N}^0$: 1.4 kJ mol⁻¹); formycin A ($\Delta\Delta G_{P-N}^0$: 2.0 kJ mol⁻¹); formycin B ($\Delta\Delta G_{P-N}^0$: 1.4 kJ mol⁻¹ and $\Delta\Delta G_{D-N}^0$: –0.2 kJ mol⁻¹)] and purine *N*-nucleosides [β-D-A ($\Delta\Delta G_{P-N}^0$: 3.0 kJ mol⁻¹); β-D-G ($\Delta\Delta G_{P-N}^0$: 3.0 kJ mol⁻¹ and $\Delta\Delta G_{D-N}^0$: –1.3 kJ mol⁻¹)].

(C) Tunable *gauche* Effect

Conformational analyses with of 2′-deoxy-2′-substituted uridine[7c] and adenosine[7d] derivatives showed qualitatively that the population of N-type pseudorotamers linearly increases with increasing electronegativity of the 2′-substituent as a result of the enhanced 2′-GE. 2′-Thionucleosides[7d,3a] prefer more S-type geometries than in 2′-deoxynucleosides. Similarly, the two-state N ⇌ S equilibrium in 2′-methylthionucleosides[7f] is strongly (>70%) biased toward S-type conformations in CD₃OD, and the effect of 2′-SMe has been attributed both to its reduced electronegativity (*i.e.* resulting in weaker GE[S2′–C2′–C1′–O4′] and GE[S2′–C2′–C1′–N1/9]) and increased steric bulk (resulting in the destabilization of N-type pseudorotamers).

Similarly electronegative nature of 3′-substituent (X) dictates 3′-GE[X3′–C3′–C4′–O4′][2d,3a]. The population of S-type pseudorotamers in 3′-deoxy-3′-substituted arabinofuranosyladenine[7g] is also dictated by the tuning of the 3′-GE, which is in turn controlled by the electronegativity of the 3′-substituent (X). The temperature-dependent pseudorotational analyses of 3′-substituted (X)-β-D-ddN[2d] [where X = NH₂, OH, OMe, NO₂, OPO₃H⁻ and F] and subsequent quantitative estimation of thermodynamics of 3′GE (ΔH_{GE}^0, in kJ mol⁻¹)[2d] showed the increasing preference for *gauche* orientation within [X3′–C3′–C4′–O4′] fragment [NH₂: –2.8 < OH: –7.2 < OMe: –7.5 < NO₂: –7.8 < OPO₃H⁻: –8.0 < F: –11.3] with increasing electronic nature of 3′-substituents in terms of respective Mullay's group electronegetivity values (shown in parenthesis): X = NH₂ (3.15) < OH (3.97) < OMe (4.03) < NO₂ (4.08) < OPO₃H⁻ (4.12) < F (4.73).

(D) Competing Anomeric and *gauche* Effects

Sugar substitution dictates the AE (*e.g.* the interplay between AE and GE in β-D-dN, see Fig. 3) as the participation of stronger 3′GE causes weaker AE in β-D-dN compared to β-D-ddN and β-D-rN (Fig. 2). The GE of highly electronegative fluorine substituent, has a profound stereoelectronic effect, thereby it governs the overall conformation of the sugar ring[3a,9]. The sugar moieties in 2′-α-fluoro-2′,3′-β-D-dideoxyuridine and 3′-β-fluoro-2′,3′-β-D-dideoxyuridine adopt exclusively N-type conformations[3a], owing to the cooperative drive of the GE[F2″(α)–C2′–C1′–O4′] and GE[F3′(β)–C3′–C4′–O4′], respectively, with the AE[O4′–C1′–N1/9].

In contrast, as a result of configuration-dependent GE, the two-state N ⇌ S pseudorotational equilibrium in 2′-β-fluoro-2′,3′-β-D-dideoxyuridine and 3′-α-fluoro-2′,3′-β-D-dideoxyuridine are strongly biased to the S-type conformers because of the predominance of the [F2′(β)–C2′–C1′–O4′] and [F3″(α)–C3′–C4′–O4′] *gauche* effects, respectively, over the AE[3a]. Recent studies[7d] have shown that incorporation of 2′-deoxy-2′-fluoro-β-D-nucleoside having preferred O4′-*endo* sugar conformation in a DNA/RNA hybrids duplex invoke improved nuclease resistance and RNase H digestion of DNA/RNA hybrid duplex, indicating the importance of 2′GE directed preferred sugar N-type conformation in duplex stability as well as RNase H activation.

In β-D-rN, the sugar conformation is driven by the interplay of the following stereoelectronic *gauche* effects besides the anomeric effect:
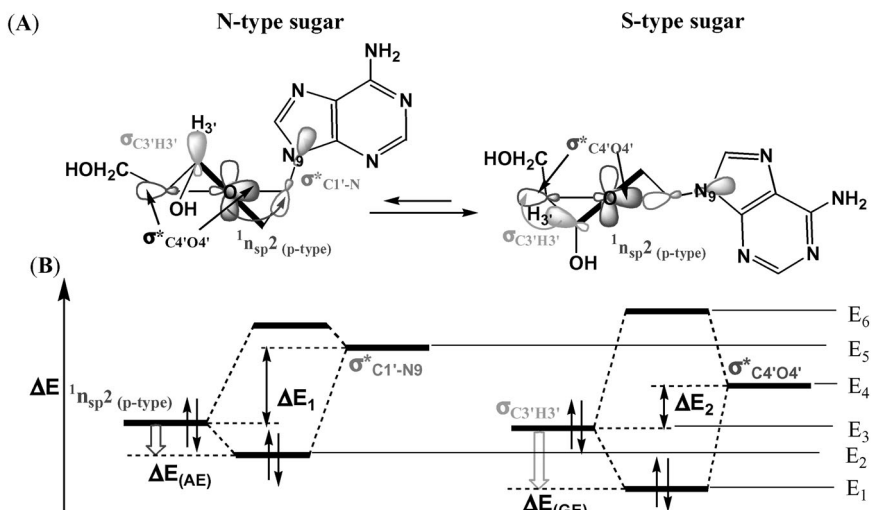
The relative energies of orbitals (E_1 - E_6) are based on their relative donor- acceptor abilities, and they can be modulated by the nature of the substituent

FIG. 3
The interplay of the AE and the GE[HO3′-C3′-C4′-O4′] in β-D-dNs to drive the N ⇌ S equilibrium. (**A**) $^1n_{sp2}$ $\sigma^*_{C1′N1/9}$ orbital overlap (*i.e.* AE) favours N-type conformation, whereas $\sigma_{C3′H3′}$ $\sigma^*_{C4′O4′}$ interactions (*i.e.* 3′GE) stabilize S-type conformations. (**B**) The energy difference between $\sigma_{C3′H3′}$ and $\sigma^*_{C4′O4′}$ (ΔE_1) is smaller (hence a better orbitals overlap) than that between $^1n_{sp2}$ and $\sigma^*_{C1′N1/9}$ (ΔE_2), therefore the GE is more efficient than the AE in β-D-dN. The stereoelectronic contribution of 5′-CH$_2$OH has not been taken into consideration as it has negligible contribution in the drive of the sugar conformation[3a]

(i) GE[O4′–C2′–C1′–O2′], (ii) GE[O4′–C3′–C4′–O3′] and (iii) GE[HO2′–C2′–C1′–N1/9]. However, GE[O4′–C4′–C3′–O3′] and GE [O4′–C1′–C2′–O2′] partially cancel each other. Additionally, the GE[O2′–C2′–C1′–N1/9] involving $\sigma_{C2'-H2'}$ $\sigma^*_{C1'-N9/1}$ orbital mixing drives the pseudorotational equilibrium of the sugar moiety in β-ribonucleos(t)ides toward S-type pseudorotamers. The strength of GE[O2′–C2′–C1′–N1/9] is in the order of adenine (-7.9 kJ mol^{-1}) > guanine (-6.7 kJ mol^{-1}) > cytidine(-2.5 kJ mol^{-1})[2j,3a].

Moreover, the ability of the effect of 2′-OH to counteract the GE[O3′–C3′–C4′–O4′] by stabilizing N-type conformations increases in the order: 3′-deoxyadenosine < adenosine < adenosine-3′-monophosphate[3a] which can be attributed to the more efficient GE[O2′–C2′–C1′–O4′], or to the weakening of the GE[O2′–C2′–C1′–N9]. However, the GE[O4′–C4′–C3′–O3′PO$_3$H$^-$] is found to be less efficient by -1.4 kJ mol^{-1} in adenosine-3′-ethylphosphate than in 2′deoxyadenosine-3′-ethylphosphate (Fig. 6), thereby showing the stereoelectronic modulation of 2′-OH in the former besides its intra- and intermolecular hydrogen bonding capability[2p].

(E) Recognition of Pentose-Sugar Conformation by Various Enzymes
Methanocarba nucleosides[9a,b] having a rigid bicyclo[3.1.0]-hexane template have been instrumental in defining the role of sugar pucker by stabilizing biologically preferred sugar conformation [*e.g.* (*N*)-(+)-methanocarba-G and (*N*)-(–)-methanocarba-A are preferentially recognized as substrate of adenosine deaminase[9a]]. It has also been shown[9b] that at recombinant human P2Y$_1$ and P2Y$_2$ receptors, (*N*)-methanocarba-ATP with N-type sugar conformation, was 138- and 41-fold more potent than racemic (*S*)-methano-ATP with S-type sugar conformation, as antagonists.

Recent NMR studies[2q] with ^{13}C/^{2}H double-labelled 2′-deoxyadenosine (dAdo) and the corresponding 2′-deoxycytidine (dCyd) moieties in the complexes with human recombinant deoxycytidine kinase (dCK) showed that the ligand (*i.e.* dCyd and dAdo) adopts an S-type sugar conformation when bound to dCK endowing the importance of stereoelectronic force dependent sugar conformation in forming kinetically favored enzyme complex.

(F) RNA Molecular Wire
The 3′-ethylphosphate, 5′-methylphophate derivatives of guanosine (EtpGpMe, **1**)[2n], adenosine (EtpApMe, **2**)[2o] and cytosine (EtpCpMe, **3**) in conjuction with their abasic (Ab) counterpart [Etp(Ab)Me, **4**][2n] can be considered as a mimicking model of trinucleoside diphosphate (Fig. 1). The comparative pH-dependent conformational analyses has been performed to shed light on how the strength of intramolecular stereoelectronic effects is modulated by the change of protonation $\rightleftarrows$ deprotonation equilibrium of

the aglycone in absence of any intramolecular base-base stacking. It shows a complete interdependency of conformational preference of sugar and phosphate backbone as the protonation $\rightleftharpoons$ deprotonation equilibrium of the aglycone changes as a function of pH.

In oligonucleotides the protonation and/or methylation of nucleobase directly affects their hydrogen-bonding capabilities and therefore induces change in overall three-dimensional structure[3a,10]. In this study we have shown that changing the electronic character of aglycone through protonation at basic site (*i.e.* N7 of guanin-9-yl, N1 of adenin-9-yl and N3 of cytosin-1-yl) not only modulates the shift of N $\rightleftharpoons$ S pseudorotational equilibrium of their constitute sugar by strengthening the anomeric effect but is also transmitted to the sugar-phosphate backbone to influence the conformation of backbone in **1**–**3**. This tunable transmission, compared to the abasic counterpart [Etp(ab)pMe, **4**], is found to be much stronger at the 3′-phosphate compared to 5′-end.

The N $\rightleftharpoons$ S pseudorotational equilibria in **1** and **2** are gradually shifted towards N-type pseudorotamers [79% S (for **1**) and 76% S (for **2**) in neutral state to 55% S (for **1**) and 67% S (for **2**) in protonated state][2n,o] as reflected from change of ΔG^0 (at 298 K) from –3.3 kJ mol^{-1} (for **1**) and –2.8 kJ mol^{-1} (for **2**) in neutral state to –0.1 kJ mol^{-1} (for **1**) and –1.7 kJ mol^{-1} (for **2**) in protonated state (Fig. 4B).
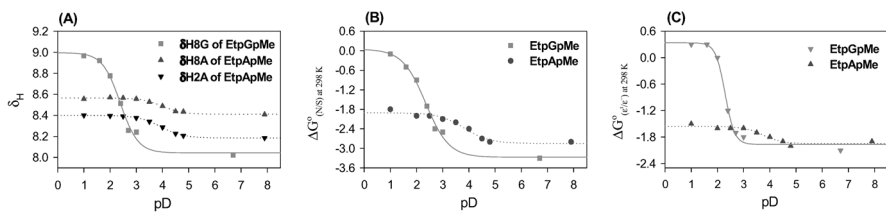

FIG. 4

Panel (**A**) shows the plots of H8 chemical shift of the constituent guanine-9-yl nucleobase (δH8G in ppm) in **1** as well as H8 and H2 chemical shift of the constituent adenin-9-yl nucleobase (δH8A and δH2A, respectively, in ppm) in **2**, as a function of pD at 298 K. Panels (**B**) and (**C**) show the plots of the experimental ΔG^0 (in kJ mol^{-1}) of the N $\rightleftharpoons$ S equilibrium[2,3,6] of the constituent pentofuranose moiety and that of $\varepsilon^t \rightleftharpoons \varepsilon^-$ equilibrium of the 3′-ethylphosphate group in **1** and **2**, respectively, as a function of pD at 298 K. The following pK_a values have been obtained: 2.4 ± 0.1 (for δH8 in **1**), 4.0 ± 0.1 and 3.9 ± 0.02 (for δH8 and δH2, respectively, in **2**) in Panel (**A**); 2.4 ± 0.1 (for **1**) and 3.8 ± 0.2 (for **2**) in Panel (**B**); 2.3 ± 0.04 (for **1**) and 3.7 ± 0.2 (for **2**) in Panel (**C**)

The conformational bias across C3′–O3′ bond (ε torsion, C4′–C3′–O3′–P) is interpreted in terms of two-state $\varepsilon^t \rightleftharpoons \varepsilon^-$ equilibrium[2n,o] as analysed by ^{1}H NMR. The population of ε^- (at 298 K) decreases from 69% (for **1**) and 68% (for **2**) in neutral state to 48% (for **1**) and 65% (for **2**) in protonated state. The corresponding shift of ΔG^0 of $\varepsilon^t \rightleftharpoons \varepsilon^-$ equilibrium is from –2.1 kJ mol^{-1} (for **1**) and –1.9 kJ mol^{-1} (for **2**) in neutral state to +0.3 kJ mol^{-1} (for **1**) and –1.5 kJ mol^{-1} (for **2**) in protonated state. Interestingly, the sigmoidal plot of pD-dependent ΔG^0 values for the N $\rightleftharpoons$ S as well as $\varepsilon^t \rightleftharpoons \varepsilon^-$ equilibria in **1** and **2** (Fig. 4B) has almost identical pK_a to that of constituent guanin-9-yl and adenin-9-yl nucleobase respectively, as determined independently from the plot of pD-dependent H8 and/H2 chemical shift (Fig. 4A). Thus, the pD-dependent reorientation of the 3′-ethylphosphate moiety across the C3′–O3′ bond is directly dictated by the pK_a of the constituent aglycone in **1** and **2**.

The cooperative shift of the (N,ε^t) $\rightleftharpoons$ (S,ε^-) equilibrium as the result of protonation of aglycone in **1** and **2** is evidenced by the straight line obtained from the plot of pD-dependent $\Delta G^0_{(N/S)}$ as a function of pD-dependent $\Delta G^0(\varepsilon^t/\varepsilon^-)$ (Fig. 5A) as well as from plot of $\Delta G^0(\varepsilon^t/\varepsilon^-)$ and $\Delta G^0_{(N/S)}$ as a function of δH8 and δ^{31}P , respectively (Figs 5B and 5C).

This shows that as the constituent guanin-9-yl nucleobase is gradually protonated in the acidic medium, the modulation of the strength of the AE shifts the N $\rightleftharpoons$ S equilibrium toward N-type conformer, which in turn dynamically shifts the $\varepsilon^t \rightleftharpoons \varepsilon^-$ equilibrium toward more ε^t in comparison with
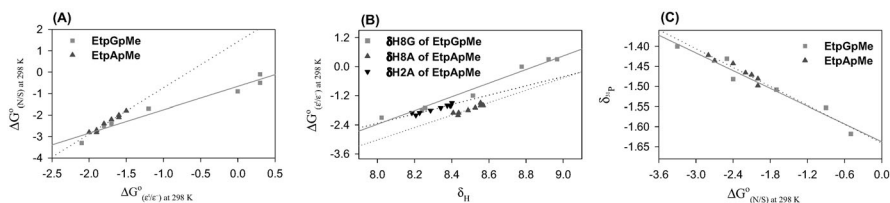

Fig. 5

Panel (**A**) shows the plot of ΔG^0 (in kJ mol^{-1}) of the N $\rightleftharpoons$ S pseudorotational equilibrium[2,3,6] as a function of the ΔG^0 (in kJ mol^{-1}) of $\varepsilon^t \rightleftharpoons \varepsilon^-$ equilibrium of the 3′-ethylphosphate group at 298 K for **1** and **2**; R = 0.98 (for **1**) and 0.98 (for **2**). Panel (**B**) shows the plot of ΔG^0 (in kJ mol^{-1}) of the $\varepsilon^t \rightleftharpoons \varepsilon^-$ equilibrium[2n,o,3a] as a function of the chemical shift of the constituent guanine-9-yl nucleobase (δH8G in ppm) in **1** as well as H8 and H2 chemical shift of the constituent adenin-9-yl nucleobase (δH8A and δH2A respectively in ppm) in **2** at 298 K; R = 0.99 (for **1**), 0.94 and 0.97 (for δH8A and δH2A respectively in **2**). Panel (**C**) shows the plot of ΔG^0 (in kJ mol^{-1}) of the N $\rightleftharpoons$ S pseudorotational equilibrium[2,3,6] as a function of the phosphorous chemical shift (δ^{31}P in ppm) for **1** and **2** at 298 K; R = 0.97 (for **1**) and 0.96 (for **2**)

the neutral state. It is noteworthy that the proof of this transmission of electronic information in **1** and **2** (*i.e.* from nucleobase to phosphate through sugar) is evident by the fact that the pK_a values of the corresponding aglycones [2.4 for guanin-9-yl and 3.9 for adenin-9-yl in **1** and **2**, respectively] are the same as the β-D-ddN, β-D-dN and β-D-rN within the error limits of our experimentals[2n,o].

As a control experiment, the difference in $^3J_{HH}$, $^3J_{HP}$ and $^3J_{CP}$ coupling constant values between neutral and acidic pDs at 298 K was found to be negligible in apurinic phosphodiester **4**, showing that owing to the absence of aglycone, the N $\rightleftarrows$ S equilibrium as well as conformation across C3′–O3′ remain unbiased at all pDs compared to **1** and **2**.

This result constitutes the first experimental evidence for transmission of electronic information to steer the conformation of the 3′-phosphate moiety as a result of change of electronic properties of the nucleobase (protonation/deprotonation) *via* the tuning of the sugar conformation in a nucleoside 3′,5′-bisphosphate.

However, this aglycone dependent conformational transmission of sugar-phosphate backbone *via* pentofuranose depends upon the tunability of aglycone vis-à-vis conformational modulation of sugar geometry. Our control studies with EtpCpMe (**3**) at neutral and protonated state showed that the relative conformational tunability is in order EtpGpMe (**1**) > EtpApMe (**2**) > EtpCpMe (**3**) (Fig. 6).
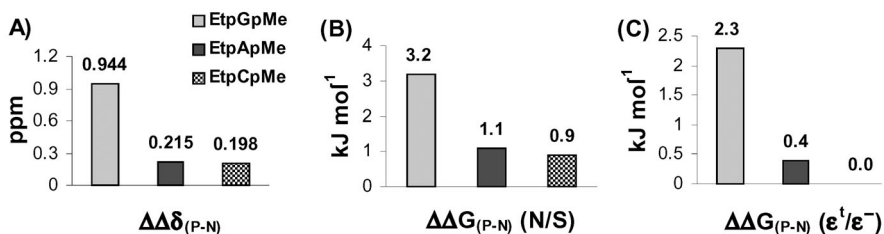
FIG. 6

The relative conformational tunability of EtpGpMe (**1**), EtpApMe (**2**) and EtpCpMe (**3**) between neutral (N) and protonated (P) state at 298 K. Panel (**A**) shows the relative change of chemical shift of aromatic protons [$\Delta\Delta\delta_{(P-N)}$] in **1**–**3**; Panel (**B**) and (**C**) show the relative change of free energy of the N$\rightleftarrows$S pseudorotational equilibrium [$\Delta\Delta G^0_{(P-N)}$ (N/S), in kJ mol^{-1}] and that of $\varepsilon^t\rightleftarrows\varepsilon^-$ equilibrium [$\Delta\Delta G^0_{(P-N)}$ ($\varepsilon^t/\varepsilon^-$), in kJ mol^{-1}] in **1**–**3**. The relative order of tunability is **1** > **2** > **3**

2. The Substitution of a Pentose-Sugar Moiety of the 2′-Deoxyadenosine Residue by a Carbocyclic Analogue, as in 2′-Deoxyaristeromycin, in a Self-Complementary 12mer Results in to Two Dynamically Interconverting Hoogsteen Type and Watson–Crick Basepaired Duplexes in Dynamic Equilibrium, Compared to the Native Duplex, which Entirely Adopts a Typical B-Type DNA Conformation

In order to understand the structural significance of endocyclic O4′ in the pentofuranose moiety, we have prepared an analog of a Dickerson–Drew dodecamer, $5'$-d(C^{1}G^{2}C^{3}G^{4}A^{5}A^{6}T^{7}T^{8}C^{9}G^{10}C^{11}G^{12})$_2$-$3'$ (duplex **1**), in which the pentose-sugar moiety of the 2′-deoxyadenosine residue A^6 (Fig. 7A) has been replaced by a carbocyclic analogue, 2′-deoxyaristeromycin, $\underline{A}^6$ (Fig. 7B). The result of the solution conformation studies[11] of duplex **1** by NMR showed that it consisted of two dynamically interconverting duplexes, (**1A**) $\rightleftarrows$ (**1B**). Upon comparison with the native duplex (**2**), it was found that duplex (**1A**) has a conformation that is identical to the native (**2**)[12,13]. On the other hand, in the (**1B**) form, the basepairs formed between $\underline{A}^6$ and T^7 at the center of the duplex are of Hoogsteen type (Fig. 8B), while the rest of the duplex has Watson–Crick basepairing (Fig. 8A), adopting a typical B-type conformation[12,13]. The big changes in the chemical shifts observed for the central $\underline{A}^6$ and T^7 residues (as well as for the neighbouring A^5 and T^8) in duplex (**1B**) indicated that there is a major change in base stacking at the centre of the duplex, which could not explained by a standard Watson–Crick basepaired B-type DNA duplex. That this is indeed owing to Hoogsteen basepairing is evident from the following observations: (i) Duplex (**1B**) had NOESY crosspeaks between H3T^7 and H8$\underline{A}^6$, H3T^7 and H1′A^6 and between H3T^8 and H8$\underline{A}^6$, which is consistent with what is expected from Hoogsteen basepairing (Fig. 8B), as found in the earlier base triple
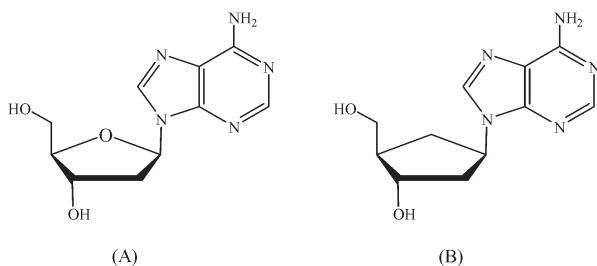

(A)   (B)

Fɪɢ. 7
The structures of 2′-deoxyadenosine (A) and 2′-deoxyaristeromycin (B)

DNA[14]. (ii) The H8–H1′ crosspeak of $\underline{A}^6$ assigned to duplex (**1B**), had a much quicker NOE buildup, with a 6–7 fold larger intensity at *ca* 70 ms mixing time (Fig. 8C) than the corresponding crosspeak in the fully Watson–Crick basepaired duplex (**1A**), which suggests a *syn* conformation for the former. (iii) The observed NOE crosspeak between H8A[5] to H2$\underline{A}^6$, together with the interruption in the aromatic–aromatic connectivity between A[5] and $\underline{A}^6$, indicates *syn* conformation (see above). (iv) Finally, we observed temperature-dependent exchange peaks in ROESY and NOESY spectra between the resonances belonging to duplexes (**1A**) and (**1B**), showing that the two conformers exist in a dynamic interconverting equilibrium.

Thus, duplex (**1**) exists in two dynamically interconverting conformations: *a fully* Watson–Crick basepaired DNA duplex (**1A**) and a doubly A[6]:T[7] Hoogsteen basepaired (**1B**) B-type DNA duplex. The thermodynamics of the equilibrium of (**1A**) $\rightleftarrows$ (**1B**): $K_{eq} = k_1/k_{-1} = 0.56 \pm 0.08$. The dynamic conversion of the *fully* Watson-Crick basepaired (**1A**) to the *partly* Hoogsteen basepaired (**1B**) structure is marginally kinetically and thermodynamically disfavoured [k_1 (298 K) = 3.9 $\pm$ 0.8 s^{-1}; $\Delta H^{0\ddagger}$ = 164 $\pm$ 14 kJ mol^{-1}; $-T\Delta S^{0\ddagger}$ (298 K) = –92 kJ mol^{-1} giving a $\Delta G^{0\ddagger}_{298}$ of 72 kJ mol^{-1}. E_a (k_1) = 167 $\pm$ 14
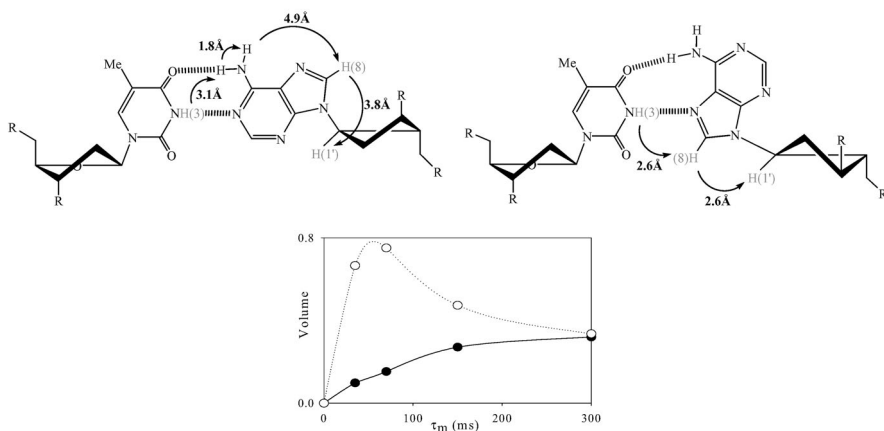
FIG. 8

Schematic view of two A-T basepairs showing various key distances amongst imino-amino-aromatic-sugar H1′ in a Watson–Crick (A) vis-à-vis a Hoogsteen (B) basepair[13a,14]. (C) The quicker NOE buildup (dotted line) for the H8A[6]-H1′A[6] NOE belonging to the Hoogsteen basepaired duplex (**1B**) indicates a *syn* conformation, compared to the native H8A[6]-H1′A[6] NOE in the native duplex (plain line). The H8A[6]-H1′A[6] NOE volume of each duplex has been normalised against its H5-H6 crosspeak of C[3] residue

kJ mol^{-1}] compared to the reverse conversion of the Hoogsteen (**1B**) to the Watson–Crick (**1A**) structure [k_{-1} (298 K) = 7.0 ± 0.6 s^{-1}, $\Delta H^{0\ddagger}$ = 153 ± 13 kJ mol^{-1}; $-T\Delta S^{0\ddagger}$ (298 K) = –82 kJ mol^{-1} giving a $\Delta G^{0\ddagger}_{298}$ of 71 kJ mol^{-1}. E_a (k_{-1}) = 155 ± 13 kJ mol^{-1}]. A comparison of $\Delta G^{0\ddagger}_{298}$ of the forward (k_1) and backward (k_{-1}) conversions, (**1A**) $\rightleftarrows$ (**1B**), shows that there is *ca* 1 kJ mol^{-1} preference for the Watson–Crick (**1A**) over the double Hoogsteen basepaired (**1B**) DNA duplex.

A small change in one sugar residue (the O4' oxygen replaced by CH$_2$) has a dramatic effect on the local structure and flexibility of a B-type DNA duplex[11]. The duplex is in an equilibrium between a typical fully Watson–Crick basepaired B-DNA like structure and a structure in which the two central basepairs ($\underline{A}^6$-T^7/T^7-$\underline{A}^6$) are Hoogsteen basepaired, while all others are Watson–Crick basepaired in a B-DNA like structure. However, this change does not seem to induce any large changes in the stability of the duplex as characterised by its melting temperature and thermodynamics. The main effect of the Hoogsteen basepairs on the overall structure is ~2–3 Å narrowing of the minor groove and a corresponding widening of the major groove (Fig. 9). To form a Hoogsteen basepair the 2'-deoxyadenosine moiety must change from *anti* to *syn* conformation: The replacement of the endocyclic 4'-oxygen in the natural pentose sugar with a methylene group makes the stereoelectronic anomeric and *gauche* effects in the resulting
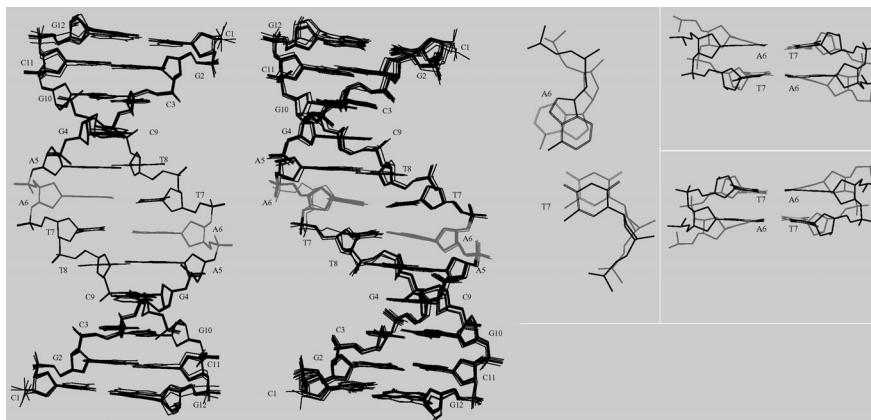

FIG. 9
(A) Superimposition of 8 representative Watson–Crick basepaired duplex structures after refinement (**1A**) [RMSD = 0.33 Å]. (B) Superimposition of 8 representative Hoogsteen basepaired duplex structures after refinement (**1B**) [RMSD = 0.38 Å]. (C) Zooms of the two central basepairs

carbocyclic ring disappear, thereby making it more flexible. Additionally, the steric clash between the 4′-oxygen and the aglycone present in the O4′-*endo* conformation in the natural pentofuranose ring is not present in the carbocyclic counterpart, thereby making the *syn/anti* conformational transition more facile in the latter, promoting the Hoogsteen basepairing. It is interesting to note that only very few changes, mainly in α, δ and γ torsions[11], in the sugar-phosphate backbone seem to be necessary to accommodate the Hoogsteen basepairing.

It has recently been shown that a single 2′-deoxyaristeromycin (A) substitution does not significantly alter the structure of an asymmetric DNA duplex[15]. In our self-complementary and symmetric DNA duplex[11], this situation has however changed dramatically: The local structure at the center of a palindromic DNA sequence changes because the two A substitutions on the opposite strands are brought into close proximity of each other, thereby giving rise to an increased flexibility at the center which seems to be necessary for the bases to flip over from *anti* to *syn* and form the Hoogsteen basepairs. Further, the existence of the Hoogsteen basepaired conformer shows that this is not simply owing to the intrinsic flexibility of the duplex; this is albeit the result of local structural changes orchestrated by the primary sequence as well as by the site of the modified A residue in our duplex, prompting the helix to be stabilised by *syn A/anti T* basepairing. This is also supported by the fact that the bases of the two modified A residues *always co-flip* to give either two *syn* or two *anti* A^6-T^7 basepairing. As a result, we see a dynamic equilibrium of *ca* 1:1 mixture of Hoogsteen and Watson–Crick basepaired duplexes. It is noteworthy that there is no detectable presence of any species where the base of the A^6 residue of one strand is in *syn* conformation and the one of the opposite strand is in *anti*.

In an experiment, where 2′-deoxyaristeromycin has been incorporated in both residue A^5 and A^6 in the same duplex (data not shown), as many as 4 major substructures can be observed in NMR under the same conditions.

The above data shows that (i) there is very little energetic preference for the pentofuranose-based DNA compared to the carbocyclic counterpart; (ii) the free-energies for forming the Watson–Crick and the Hoogsteen basepaired duplexes are very similar because there is very little energetic discrimination for the carbocyclic vis-à-vis pentofuranose world, and (iii) this shows the limitations of 2′-deoxyaristeromycin-incorporation in DNA duplexes in order to increase nuclease stability as we can see how the structure of the DNA duplex starts to get disordered as the number of modified residues close to each other increases, (iv) the natural preference for the pentofuranose based nucleic acids over carbocyclic counterparts is presum-

ably based on controlling the DNA polymorphism in a punctuated manner, dictated by a relatively higher energy barrier in the former (2–4 kJ mol^{-1}) compared to the latter.

3. The Sensitivity of the RNase H Discriminates the Local Structure Changes Owing to Conformational Transmission Induced by N-type or N/E-Type Sugar Constrained Nucleotides in the Antisense Strand of the Antisense-RNA Hybrid Duplex

RNase H, an ubiquitous enzyme, cleaves the RNA in a DNA/RNA hybrid[16]. Based on the dissociation constant determined by competitive inhibition analysis[17], the RNase H can bind to all duplexes, irrespective of their conformational preorganization [DNA/RNA > RNA/RNA > DNA/DNA]. The catalytic cleavage by the enzyme however demands a *flexible* hybrid duplex structure whose overall geometry should be close to an A type helix[16]. For example, in the native DNA-RNA duplex, the conformation of the DNA strand is B type (all nucleotides are in O4′-*endo* conformation) whereas the RNA strand adopts a conformation which is very similar to single stranded A-RNA type (all nucleotides are in C3′-*endo* conformation)[18]. It has emerged that the RNase H cleavage site retains this B-type-DNA/A-type RNA conformation in order to be substrate for cleavage reaction by RNase H[18]. This conformational criterion has been so far difficult to achieve with the modified residues in the antisense strand at the cleavage site. We have thus witnessed the emergence of the gapmer or the mixmer strategies, which not only allows the cleavage of the complementary RNA strand, but also enhances the thermodynamic stability of the hybrid duplex[17,19]. The tolerance of the modified nucleotide residues in the antisense strand in the above two strategies are very sensitive to the *type of modifications used*, both because of *conformational pre-organization* and the *intrinsic flexibility* required of the hybrid duplex for catalytic cleavage by RNase H[16].

Most of the North conformationally constrained nucleosides upon introduction (full modification or partial modification) to Antisense Oligo-Nucleotide (AON) render their hybrid duplex with RNA (AON/RNA) to a rigid RNA/RNA type duplex, which were found to be insensitive towards the RNase H promoted cleavage, although the stability of the resulting hybrid duplexes are enhanced[19]. The reason for this RNase H insensitivity of the AON/RNA hybrid duplex containing conformationally-constrained nucleotides, both in the gapmer as well as in the mixmer strategies, is beginning to be understood[16]. Remarkably, some conformational alterations brought about by the structural modifications are transmitted to steer the

conformation of the neighboring nucleotides, which alter the microscopic structure of the hybrid, and is indeed sensed by RNase H, but insensitive to spectroscopic techniques such as NMR or CD[20]. A slow consensus is however emerging as to how far the rigidity of the N- or N/E-type conformationally constrained nucleotides in the AON can propagate to alter the conformational characters of the neighboring S-type residues in the hybrid duplex. This information is important because the alteration of S-type character in the neighbors to an N-type or [North-East (N/E)-type] pseudorotamer forces those nucleotides in the AON/RNA duplex to adopt a pseudo RNA/RNA type conformation, which is not recognized for cleavage by RNase H. Our latest result however show that this pseudo RNA/RNA type conformational patches in the hybrid duplex is however recognized by RNase H for binding. The uniqueness of RNase H promoted cleavage of AON/RNA hybrids holding varying number of conformationally constrained North-East (N/E)-type nucleotides can be employed to address these issues which we have shown recently with the oxetane incorporated nucleotides in the antisense-RNA hybrid duplex[20].

We have introduced single, double, triple N/E conformationally constrained nucleoside, [1-(1′,3′-O-anhydro-β-D-psico-furnosyl)thymine] (**T**), to a 15 mer AON and targeted to a 15 mer RNA. CD failed to detect any structural perturbances of the modified hybrids compared to the native counterpart; however, the RNase H cleavage pattern of these hybrid duplexes clearly showed the changes local conformation spanning a total of 5 nucleotides including the modification towards the 5′-end of AON (3′-end of RNA). This was evident from the fact that the 5-nucleotide region of the RNA strand, beginning from the nucleotide opposite to the **T** modification, became completely inactive to the catalytic cleavage reaction by RNase H[20]. Since the sites just after the 5 nucleotides were accessible for enzymatic cleavage (Fig. 10), and the fact that the binding and cleavage sites are different for RNase H[21], it is evident that the structurally altered duplex region was suitable for the enzyme binding but not for cleavage. By suitably placing the just three **T** modifications we have shown that the single cleavage site in the RNA strand can be successfully engineered in the 15mer AON/RNA hybrid duplex. (Fig. 10) without loosing any overall cleavage activity. This work clearly shows that introduction of the N- and/or N/E-type conformational constraint at the oligonucleotide level leads to microenvironmental conformational alterations in the neighboring 4 nucleotides toward the 5′-end of the AON strand, which alters the conformation of the duplex to pseudoRNA/RNA type hybrid duplex. This conformational transmission can be effectively mapped by RNase H, when CD and NMR fails to
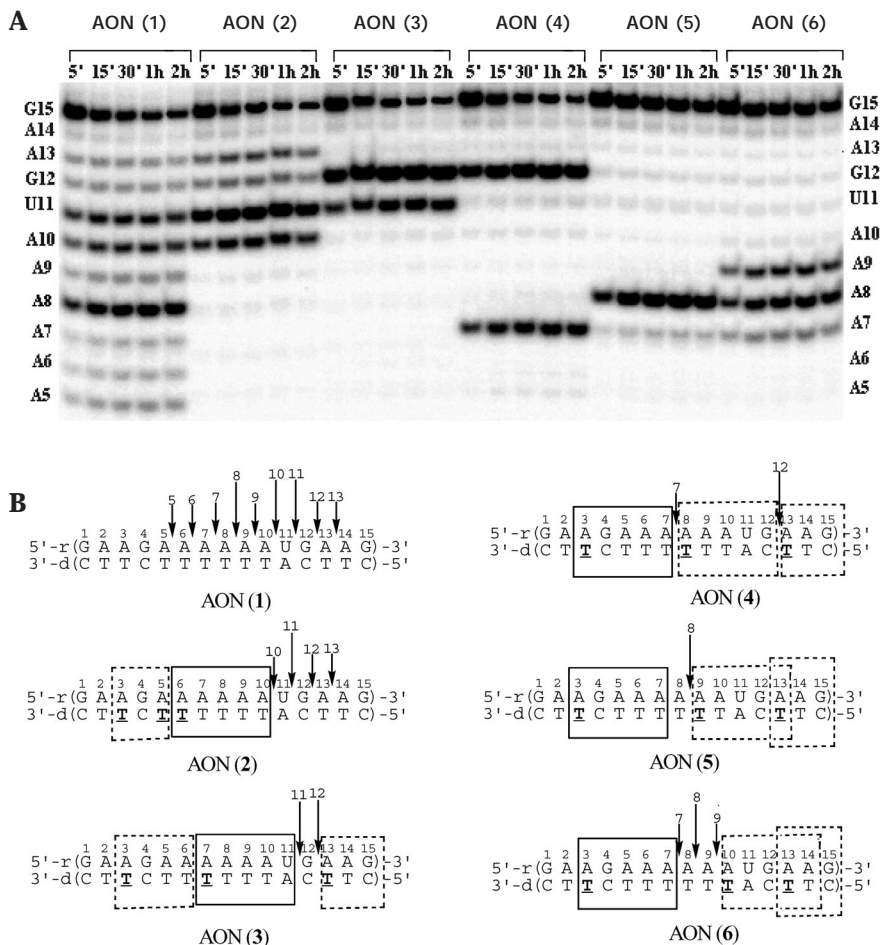
FIG. 10
(A) The PAGE analysis of RNase H hydrolysis of the hybrid duplexes, AON (1)–(6)/RNA. Time after the addition of the enzyme is shown on the top of each gel lane. The length and sequence of 5'-^{32}P-labeled RNAs formed up on enzymatic cleavage are shown on the left and right side of the gel and it was deduced by comparing the migration of products with those oligonucleotides generated by partial digestion of the target RNA by snake venom phosphodiesterase (SVPDE). (B) RNase H cleavage pattern of the hybrid duplexes. Long and short arrows represent major and minor sites respectively (after 2 h of incubation). Boxes represent the parts of the RNA sequence insensitive towards RNase H cleavage

show any conformational heterogeinity in the local structure. Thus this constitutes an effective means to map the local conformation of the hetero-duplex by RNase H.

There is only limited information available regarding the tolerance of RNase H towards local conformational transmission of AONs holding other conformationally constrained nucleotides. A recent report[22] however out-lined the RNase H tolerence of AON/RNA hybrids modified with North-conformationally constrained LNA monomers. Introduction of one LNA it-self was found to alter global helical structure[23] (detected by CD) and three LNA monomers were sufficient to create a RNA/RNA type AON/RNA hybrid duplex. None of these modifications are however reported to elicit any RNase H response, although considerable enhancement in the thermody-namic stability was observed. Mixmer AONs with 3-5 deoxynucleotide gaps were found to be also insensitive towards RNase H promoted cleavage once hybridized to RNA[22]. This clearly showed that microstructural alterations brought by the LNA modification propagates beyond 5 nucleotides stretch, in contradistinction to our oxetane modifications[20].

The question to be addressed is how far down the polynucleotide chain the conformational transmission propagates in the LNA-modified AON/RNA hybrid duplex[20]. Clearly, an appropriate answer should open the door for the use of the LNAs both as T_m enhancer as well as a substrate for RNAse H. This has now been achieved through a systematic study with a series of LNA incorporated AON-RNA duplexes in which the size of the deoxy-nucleotide gap (required for RNase H cleavage) in the mixmer as well as in the gapmer was varied[22]. It was observed that the gapmer/mixmer of LNA/RNA duplexes having 6 to 10 deoxynucleotide gaps were cleaved by the en-zyme. Quite expectedly[20], it was also found that the maximum cleavage ef-ficiency was observed as the size of the deoxynucleotide gap was increased to 10, whereas the cleavage was observed even when the gap contains 6 nt stretch, presumably because of adaptation of substantial degree of DNA/RNA type structure[22]. This shows that the conformational transmission of LNA stretches up to 7 nucleotides (including the modification) to make it conform to RNA/RNA type structure, which is resistant to RNase H, whereas for oxetane modifications, we have shown it stretches upto 5 nucleotides[20].

The third case of conformational transmission can be found in case of AONs containing 2′-O-methylnucleosides. 2′-O-Methylnucleosides ($^3J_{1'2'}$ = 5.2 Hz, $^3J_{3'4'}$ = 4.7 Hz) show a slightly preferred N-type conformation in the North-South pseudorotational equilibrium. This slight preference for N-type conformation is attributed to the steric repulsion between the aglycone and the 2′-O-methyl group in the C2′-endo (South form)[24]. In the

AON, there would be additional steric clash of 2′-*O*-alkyl group with the 3′-phosphate, which drives it to more preferred North conformation. Therefore, unlike the other North-constrained nucleotides (LNA, oxetane...), the conformational influence by 2′-*O*-alkyl nucleotides, which can be detected by RNase H, to the neighbours are *less* pronounced, and it was found to be sequence-dependent[25]. This is clearly visible in the RNase H digestion pattern of 2′-*O*-alkyl modified AON/RNA gapmer hybrids, where the microstructural alterations brought by the 2′-*O*-methylnucleoside modification which blocks the cleavage was found to vary from 3 to 5 nucleotides including the modification[25]. This means that the conformational transmission of the North-type 2′-*O*-alkylnucleotides in the AON/RNA/RNase H ternary complex is less pronounced than in other conformationally constrained AON containing counterparts.

REFERENCES AND NOTES

1. a) Saenger W.: *Principles of Nucleic Acid Structure*. Springer Verlag, Berlin 1988; b) Tinoco I., Jr.: *J. Phys. Chem.* **1996**, *100*, 13311; c) Belmont P., Constant J. F., Demeunynck M.: *Chem. Soc. Rev.* **2001**, *30*, 70.

2. a) Koole L. H., Buck H. M., Nyilas A., Chattopadhyaya J.: *Can. J. Chem.* **1987**, *65*, 2089; b) Plavec J., Tong W., Chattopadhyaya J.: *J. Am. Chem. Soc.* **1993**, *115*, 9734; c) Plavec J., Thibaudeau C., Viswanadham G., Sund C., Chattopadhyaya J.: *J. Chem. Soc. Chem. Commun.* **1994**, 781; d) Thibaudeau C., Plavec J., Garg N., Papchikhin A., Chattopadhyaya J.: *J. Am. Chem. Soc.* **1994**, *116*, 4038; e) Plavec J., Thibaudeau C., Chattopadhyaya J.: *J. Am. Chem. Soc.* **1994**, *116*, 6558; f) Plavec J., Thibaudeau C., Viswanadham G., Sund C., Sandstrom A., Chattopadhyaya J.: *Tetrahedron* **1995**, *51*, 11775 and references therein; g) Thibaudeau C., Plavec J., Chattopadhyaya J.: *J. Org. Chem.* **1996**, *61*, 266; h) Plavec J., Thibaudeau C., Chattopadhyaya J.: *Pure Appl. Chem.* **1996**, *68*, 2137; i) Thibaudeau C., Földesi A., Chattopadhyaya J.: *Tetrahedron* **1997**, *53*, 14043; j) Luyten I., Thibaudeau C., Chattopadhyaya J.: *J. Org. Chem.* **1997**, *62*, 8800; k) Luyten I., Thibaudeau C., Chattopadhyaya J.: *Tetrahedron* **1997**, *53*, 6433; l) Thibaudeau C., Plavec J., Chattopadhyaya J.: *J. Org. Chem.* **1998**, *63*, 4967; m) Thibaudeau C., Bekiroglu S., Kumar A., Matsuda A., Marquez V. E., Chattopadhyaya J.: *J. Org. Chem.* **1998**, *63*, 5447; n) Acharya P., Trifonova A., Thibaudeau C., Földesi A., Chattopadhyaya J.: *Angew. Chem. Intl. Ed.* **1999**, *38*, 3645 and references therein; o) Velikian I., Acharya P., Trifonova A., Földesi A., Chattopadhyaya J.: *J. Phys. Org. Chem.* **2000**, *13*, 300; p) Acharya P., Chattopadhyaya J.: *J. Org. Chem.* **2001**, *67*, 1852; q) Maltseva T., Usova E., Eriksson S., Milecki J., Földesi A., Chattopadhayaya J.: *Nucleosides Nucleotides Nucleic Acids* **2001**, *20*, 1225; r) Acharya S., Acharya P., Földesi A., Chattopadhyaya J.: *J. Am. Chem. Soc.*, submitted.

3. a) For review see: Thibaudeau C., Chattopadhyaya J.: *Stereoelectronic Effects in Nucleosides and Nucleotides and their Structural Implications* (ISBN 91-506-1351-0). Department of Bioorganic Chemistry, Uppsala University Press (fax: +4618554495), Uppsala 1999 and references therein; pp. 27–29 for the two-state N $\rightleftarrows$ S pseudorotational equilibrium model as well as references 241–246 cited in this monograph; see pp. 5–23 of this monograph for the anomeric and *gauche* effects; b) de Leeuw H. P. M., Haasnoot C. A. G., Altona C.: *Isr. J. Chem.* **1980**, *20*, 108.

4. a) Petillo P. A., Lerner L. A. in: *The Anomeric effect and Associated Stereoelectronic effects* (G. R. J. Thatcher, Ed.). ACS Symposium Series, p. 156, Washington, D. C. 1993 and references therein; b) Perrin C. L., Armstrong K. B., Fabian M. A.: *J. Am. Chem. Soc.* **1994**, *116*, 715.

5. a) Dionne P., St-Jacques M.: *J. Am. Chem. Soc.* **1987**, *109*, 2616; b) Wiberg K. B.: *Acc. Chem. Res.* **1996**, *29*, 229 and references therein.

6. a) Altona C., Sundaralingam M.: *J. Am. Chem. Soc.* **1972**, *94*, 8205; b) Altona C., Sundaralingam M.: *J. Am. Chem. Soc.* **1973**, *95*, 2333.

7. a) Haasnoot C. A. G., de Leeuw F. A. A. M., de Leeuw H. P. M., Altona C.: *Rec. Trav. Chim. Pays-Bas* **1979**, *98*, 576; b) Rosemeyer H., Tóth G., Golankiewicz B., Kazimierczuk Z., Bourgeois W., Kretschmer U., Muth H.-P., Seela F.: *J. Org. Chem.* **1990**, *55*, 5784; c) Guschlbauer W., Jankowski K.: *Nucleic Acids Res.* **1980**, *8*, 1421; d) Uesugi S., Kaneyasu T., Imura J., Ikehara M., Cheng D. M., Kan L.-S., Ts'o P. O. P.: *Biopolymers* **1983**, *22*, 1189; e) Uesugi S., Miki H., Iwahashi H., Kyogoku Y.: *Tetrahedron Lett.* **1979**, *42*, 4073; f) Imazawa M., Ueda T., Ukita T.: *Chem. Pharm. Bull. (Tokyo)* **1975**, *23*, 604; g) Klimke G., Cuno I., Lüemann H.-D., Mengel R., Robins M. J. H.: *Naturforsch.* **1980**, *35c*, 853.

8. a) Polak M., Plavec J., Trifonova A., Földesi C. A., Chattopadhyaya J.: *J. Chem. Soc., Perkin Trans. 1* **1999**, 2835; b) Črnugelj M., Dukhan D., Barascut J. L., Imbach J. L., Plavec J.: *J. Chem. Soc., Perkin Trans. 2* **2000**, 255; c) Plevnik M., Črnugelj M., Štimac A., Kobe J., Plavec J.: *J. Chem. Soc., Perkin Trans. 2* **2001**, 1433; d) Rosemeyer H., Seela F.: *J. Chem. Soc., Perkin Trans. 2* **1997**, 2341.

9. a) Moon H. R., Ford H., Jr., Marquez V. E.: *Org. Lett.* **2002**, *2*, 3793; b) Kim H. S., Ravi R. G., Marquez V. E., Maddileti S., Wihlborg A., Erlinge D., Malmsjö M., Boyer J. L., Harden T. K., Jacobson K. A.: *J. Med. Chem.* **2002**, *45*, 208 and references therein; c) Ford H., Jr., Dai F., Mu L., Siddqui M. A., Nicklaus M. C., Anderson L., Marquez V. E., Barchi J., Jr.: *Biochemistry* **2000**, *39*, 2581; d) Wilds C. J., Damha M. J.: *Nucleic Acid Res.* **2000**, *28*, 3625; e) Mu L., Sarafianos S. G., Nicklaus M. C., Russ P., Siddiqui M. A., Ford H., Jr., Mitsuya H., Le R., Kodama E., Meier C., Knispel T., Anderson L., Barchi J. J., Jr., Marquez V. E.: *Biochemistry* **2000**, *39*, 11205.

10. a) Höbartner C., Ebert M., Jaun B., Micura R.: *Angew. Chem. Intl. Ed.* **2002**, *41*, 605; b) Kumar S., Horton J. R., Jones G. D., Walker R. T., Roberts R. J., Cheng X.: *Nucleic Acid Res.* **1997**, *25*, 2773.

11. Isaksson J., Zamaratski E., Maltseva T. V., Agback P., Kumar A., Chattopadhyaya J.: *J. Biomol. Struct. Dyn.* **2001**, *18*, 783.

12. Denisov A. Y., Zamaratski E. V., Maltseva T. V., Sandström A., Bekiroglu S., Altmann K.-H., Egli M., Chattopadhyaya J.: *J. Biomol. Struct. Dyn.* **1998**, *16*, 547 and references therein for references to other NMR and X-ray work on Dickerson's dodecamer.

13. a) Saenger W.: *Principles of Nucleic Acid Structure*. Springer-Verlag, New York, Berlin, Heidelberg, Tokyo 1988; b) Arnott S., Hukins D. W. L.: *Biochem. Biophys. Res. Comm.* **1972**, *47*, 1504.

14. Sklenár V., Feigon J.: *Nature* **1990**, *345*, 836.

15. Smirnov S., Johnson F., Marumoto R., de los Santos C.: *J. Biomol. Struct. Dyn.* **2000**, *17*, 981.

16. Zamaratski E., Pradeepkumar P. I., Chattopadhyaya J.: *J. Biochem. Biophys. Methods* **2001**, *48*, 189.

17. Lima W. F., Crooke S. T.: *Biochemistry* **1997**, *36*, 390.

18. Fedoroff O.-Y., Salazar M., Reid B. R.: *J. Mol. Biol.* **1993**, *233*, 509.

19. a) Manoharan M.: *Biochim. Biophys. Acta* **1999**, *117*, 1489; b) Herdewijn P.: *Biochim. Biophys. Acta* **1999**, *167*, 1489.

20. a) Pradeepkumar P. I., Zamaratski E., Földesi A., Chattopadhyaya J.: *Tetrahedron Lett.* **2000**, *41*, 8601; b) Pradeepkumar P. I., Zamaratski E., Földesi A., Chattopadhyaya J.: *J. Chem. Soc., Perkin Trans. 2* **2001**, *3*, 402. c) Pradeepkumar P. I., Chattopadhyaya J.: *J. Chem. Soc., Perkin Trans. 2* **2001**, *11*, 2074; d) Amirkhanov N. V., Pradeepkumar P. I., Chattopadhyaya J.: *J. Chem. Soc., Perkin Trans. 2* **2002**, 976.

21. Kanaya S. in: *Ribonucleases H* (R. J. Crouch, Ed.) INSERM: Paris, Chapt. 1, p. 1 (1998).

22. Kurreck J., Wyszko E., Gillen C., Erdmann V. A.: *Nucleic Acids Res.* **2002**, *30*, 1911.

23. Bodensgaard K., Petersen M., Singh S. K., Rajwanshi V. K., Kumar R., Wengel J., Jacobsen J. P.: *Chem. Eur. J.* **2000**, *6*, 2687.

24. Kawai G., Yamamoto Y., Amimura T., Masegi T., Sekine M., Hata T., Iimori T., Watanabe T., Miyazawa T., Yokoyama S.: *Biochemistry* **1992**, *31*, 1040.

25. a) Inoue H., Hayase Y., Iwai S., Ohtuka E.: *FEBS Lett.* **1987**, *215*, 327; b) Yu Y.-T., Shu M-D., Steiz J. A.: *RNA* **1997**, *3*, 324; c) Larrouy B., Boiziau C., Saproat B., Toulme J.-J.: *Nucleic Acids Res.* **1995**, *23*, 3434.